Length effect in a Co-rich amorphous wire

V. Zhukova,[1] N. A. Usov,[2] A. Zhukov,[3,4,*] and J. Gonzalez[1]
[1]*Departamento de Fisica de Materiales, Facultad de Química, Universidad del Pais Vasco, P.O. Box 1072, 20080 San Sebastián, Spain*
[2]*Troitsk Institute for Innovation and Fusion Research, 142092 Troitsk, Moscow Region, Russia*
[3]*Instituto de Ciencia de Materiales, CSIC, 28049 Cantoblanco, Madrid, Spain*
[4]*"TAMag" S.L., c/Jose Abascal 53 Madrid, Spain*
(Received 21 February 2001; revised manuscript received 16 August 2001; published 14 March 2002)

The effect of the sample length on the magnetization process of a Co-rich amorphous wire has been experimentally and theoretically studied in this paper. Experimentally it is found that the spontaneous magnetic bistability observed in a Co-rich wire is lost if the sample becomes shorter than some critical length. Such critical length is smaller than that one of Fe-rich wire. Besides, the remanent magnetization of a wire with the length less than the critical length is an increasing function of the wire length. Theoretical explanation of the observed behavior suggests that the magnetization of the inner core of the Co-rich amorphous wire, normally directed along the wire axis, may be twisted near the wire ends due to the demagnetizing field. As a result, the longitudinal component of the wire magnetization reduces gradually towards the wire ends. It is shown that the characteristic critical length for the reduction of the longitudinal magnetization component can be several orders larger than the wire radius. This estimation is in qualitative agreement with the experimental data.

DOI: 10.1103/PhysRevB.65.134407 PACS number(s): 75.50.Kj, 75.60.Ej, 75.60.Ch, 75.60.Jk

I. INTRODUCTION

The properties of amorphous ferromagnetic wires attract considerable research interest due to their unique magnetic characteristics, such as, magnetic bistability and giant magnetoimpedance effect.[1–5] A great number of experimental results for the amorphous wires were satisfactorily explained in terms of a so-called core-shell model.[6,7] In the case of a Co-rich wire with a negative magnetostriction constant, the model assumes that there is an inner core uniformly magnetized along the wire axis and an outer shell where magnetization points in the circumferential direction. Such a model explains well the magnetic bistability observed in Co-rich amorphous wires. Particularly, tensile and torsion stress dependences of the hysteresis loops of as-cast and thermally treated Co-rich amorphous wires were satisfactorily explained on the basis of the core-shell model considering the magnetoelastic anisotropy, the stress relaxation, and the induction of magnetic anisotropy by the different treatments.[8,9]

Recently this type of the magnetization distribution has been calculated theoretically for a Co-rich amorphous wire.[10] Based on the theory of viscoelasticity[11] the radial dependence of residual stress tensor components in water-quenched amorphous wire was calculated. Then the distribution of the easy anisotropy axes along the wire radius was obtained by means of a standard expression for the magnetoelastic energy density.[12] Taking into account the axial symmetry of the wire and that of the residual stresses one can prove[10,13] that the unit magnetization vector of the Co-rich wire in cylindrical coordinates (ρ,φ,z) is given by

$$\alpha_\rho = 0, \quad \alpha_\varphi = \sin\theta(\rho), \quad \alpha_z = \cos\theta(\rho), \tag{1}$$

where $\theta(\rho)$ is the angle of the unit magnetization vector with the wire axis. The function $\theta(\rho)$ is approximately zero in the core region, $\rho < R_1$, and equals $\pi/2$ in the outer shell, $R_1 < \rho < R$. Here R_1 and R are the radii of the inner core and the whole wire, respectively. The function $\theta(\rho)$ changes rapidly near the inner-core radius and describes the structure of the 90° domain wall separating the inner core and the outer shell of the wire.[10,13]

It should be noted, however, that the derivation given by Antonov *et al.*[10] and by Usov *et al.*[13] holds, strictly speaking, only for a middle part of a sufficiently long cylindrical wire. Actually, suppose for a moment that the core-shell magnetization distribution (1) remains unchanged along the wire length up to the wire ends. Then, at the ends of the wire in the inner-core region $\rho < R_1$ a surface magnetic charge arises with a density $\sigma = M_s$, where M_s is the saturation magnetization. Evidently, the demagnetizing field of the charge affects substantially the magnetization distribution near the wire ends as the anisotropy field of the wire is small. Therefore, an important question that arises is what is the characteristic length for the redistribution of the magnetization near the end of a Co-rich wire.

There is also a similar question for a Fe-rich amorphous wire having an inner core uniformly magnetized along the wire length, but for this case it was found[14–17] that the nucleation of the reversed domains takes place near the wire ends. The outer shell of Fe-rich wires has roughly radial magnetization orientation. Such significant difference in the outer shell domain structure is due to the different sign and value of the magnetostriction constant. In addition, the magnetic bistability disappears for Fe-rich wires shorter than some critical length L_z^*.[2,3,17] It was shown also that the critical length of Fe-rich wires is strongly correlated with the wire diameter, as well as with the value of the demagnetizing field. It is of the order of 70 mm for Fe-rich wires with diameter $D = 125\ \mu$m decreasing to 5 mm for $D = 10\ \mu$m.[17] For the case of the Fe-rich wire it was found from the magnetization profile measurements that this critical length is

directly correlated to the penetration depth of the reversed domains at the wire ends, L_p acting as the nucleation sites. Particularly it was found that the magnetic bistability disappears in short enough samples under conditions that the sample length $L_z = L_z^* \approx 2L_p$.

Less attention was paid to the studies of Co-rich wires. It was found that the Co-rich wire ($D = 125\ \mu$m) with a negative magnetostriction constant has magnetization profile similar to the Fe-rich wire. As in Fe-rich wires, the magnetic bistability in Co-rich wires disappears at a certain critical length, but the critical length for magnetic bistability is somehow lower than in case of the Fe-rich wire.[18]

It is important to note that the magnetostriction constant of a Fe-rich wire typically is much larger than that of a Co-rich wire.[7] In fact, a Co-rich wire with vanishing magnetostriction is an excellent example of a soft ferromagnetic media, where the decrease of the surface magnetic charge density is known to occur due to the twisting of the magnetization near the surface of a sample. For example, it was recently demonstrated by means of numerical simulation[19–21] that the magnetization curling occurs near the ends of the soft ferromagnetic particles of elongated external shape with sizes larger than the single-domain one. It is worth to note also that in the case of soft magnetic film similar effect has been justified experimentally.[22] By analogy, one can suppose that the magnetization in the inner core of a Co-rich wire is twisted near the ends of the wire in order to reduce the magnetostatic energy of the surface magnetic charge in a manner shown schematically below.

In Sec. II the experimental data on the length dependence of hysteresis loop in Co-rich amorphous wires are presented. It has been shown experimentally[16] that for the Co-rich wire the longitudinal magnetization component increases smoothly from the wire ends within the intervals of the order of several centimeters. We confirm this result and show that the magnetization profile for the water-quenched Co-rich wire with diameter $D = 125\ \mu$m depends also on the total wire length L_z. Namely, for the wire with length larger than some critical length L_z^* the longitudinal magnetization component saturates in the middle part of the wire. The critical length characterize the distance where the influence of the demagnetizing fields on the magnetization distribution within the Co-rich wire is substantial. According to experimental data for the Co-rich wire with diameter $D = 125\ \mu$m the critical length is estimated to be $L_z^* \approx 4$ cm.

The corresponding variational model is considered in Sec. III of this paper. It takes into account the magnetic anisotropy energy and the magnetostatic energy of the wire and leads to the conclusion that the longitudinal component of the magnetization averaged over the wire cross section is a function of the coordinate z along the wire length, saturating in the middle part of a sufficiently long wire. In addition, for short enough wire the remanent wire magnetization turns out to be an increasing function of the wire length.

It is also shown in Sec. IV of this paper that in qualitative agreement with the theoretical model the remanent magnetization of a Co-rich wire with $L_z < L_z^*$ is an increasing function of its length. The discussion of the results and conclusions are also given in Sec. IV.

II. EXPERIMENTAL DETAILS AND RESULTS

Water-quenched amorphous wires with 125 μm of diameter of nominal composition $Co_{72.5}Si_{12.5}B_{15}$ were kindly supplied by Unitika Ltd., Japan. The samples with lengths of 2, 3, 4, 5, 7, 10, and 12 cm were chosen for magnetic measurements. Axial hysteresis loops were obtained, at room temperature, by a conventional induction technique at a frequency of 50 Hz. The sample was placed inside Helmholtz coils that provide magnetic field of 2500 A/m in a wide region of the central zone. Two kinds of magnetic measurements were performed. In the first one the hysteresis loop was measured by a long pickup coil fixed in the center of a Helmholtz magnetizing system. In the second case a short (1-mm long) movable pickup coil was used for the local hysteresis loops measurements. Local magnetization characterization was performed by obtaining the hysteresis loop at different points (different distances from the end of the sample) along the sample using a narrow and movable secondary coil ($N = 1000$ turns, 1 mm width) along the longitudinal direction of the sample. Information obtained in this way can prove the existence of local changes of magnetization and of modifications of the domain structure. In this way a magnetization and coercivity profile were obtained.

The hysteresis loops of the amorphous wire with different length L_z of the sample measured by the first method are depicted in Figs. 1(a)–1(d). As can be observed, samples with lengths of 7, 10, and 12 cm present rectangular hysteresis loop [Figs. 1(b)–1(d)], while this squared character is lost for the sample with $L_z = 3$ cm. It should be noted that the hysteresis loop for $L_z = 3$ cm is very different from these of samples of Fe-rich wires with sample length below a critical length. Namely, Fe-rich wires with the length below the critical show two partial Barkhausen jumps, while Co-rich samples do not show such behavior.

The hysteresis loops of the amorphous wire with different lengths are depicted in Figs. 2(a)–2(c) with the local position of the secondary coil (with respect to the wire end) as a parameter. The amplitude of the applied magnetic field for the cases of $L_z = 7$ and 12 cm was just above the switching field H_s in the center of the sample.

Large Barkhausen jumps (LBJ) have been observed in samples with lengths 7 and 12 cm for the distance longer than 1.5 cm from the ends, while the rectangular character of the hysteresis loop is lost when measured closer to the ends. Note that in the case of the sample with 3 cm length the rectangular character of the hysteresis loop is lost even in the central region. In order to trace the hysteresis loops for the case of $L_z = 3$ cm, the magnetic field amplitude of 100 A/m was used [see Fig. 2(a)].

The longitudinal magnetization profiles shown in Fig. 3 were acquired from the local hysteresis loops measured for the samples of 2, 3, 4, 5, and 12 cm length. As can be observed in Fig. 3, in the samples with $L_z = 5$ and 12 cm, the length dependence of the longitudinal magnetization is quite symmetric with respect to the center of the sample. It in-

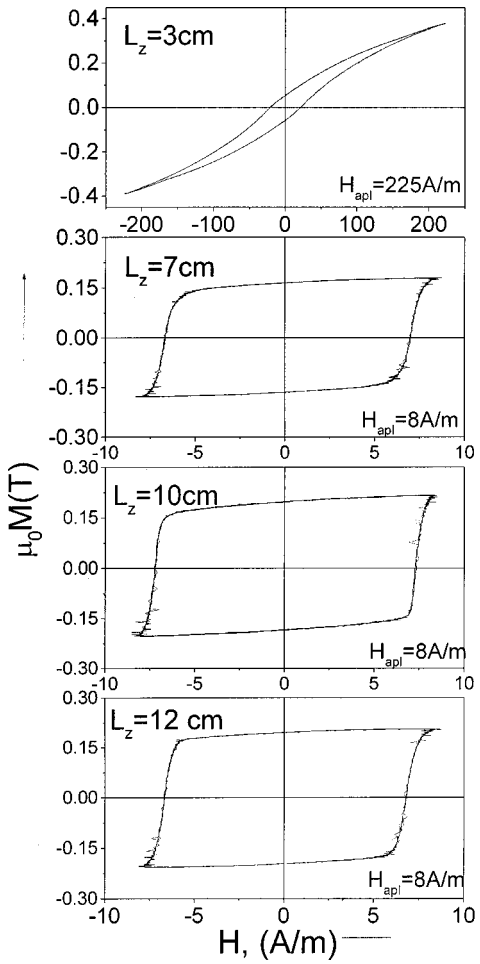

FIG. 1. Hysteresis loops of $Co_{72.5}Si_{12.5}B_{15}$ amorphous wire with sample lengths of 3, 7, 10, and 12 cm.

creases from zero (both ends) up to a roughly constant value at around 1.5 and 3.5 cm for the first sample and 2.5 and 9.5 cm for the second one, respectively. For both of the samples within the central regions the value of the longitudinal magnetization is roughly constant being about 0.14 T. It can be seen that such a roughly constant region disappears for samples with length less than 4 cm.

III. THEORETICAL MODEL

It has been shown experimentally[16] that for the Co-rich wire the longitudinal magnetization component increases smoothly from the wire ends within the intervals of the order of several centimeters.

Consider a magnetization distribution in a sufficiently short piece of the Co-rich amorphous wire. In spite of the fact that in the core region $\rho < R_1$, the easy anisotropy axis is parallel to the wire axis, the magnetization distribution within the inner core of the wire is supposed to be twisted in the manner shown in Fig. 4. As we shall see in this section, this leads to a reduction of the magnetostatic energy of surface or volume magnetic charges arising near the wire ends. For simplicity, let us suppose also that the outer shell of the wire with circumferential magnetization may not affect significantly the magnetization in the core region. Thus, in the first approximation we neglect the influence of the outer shell at all.

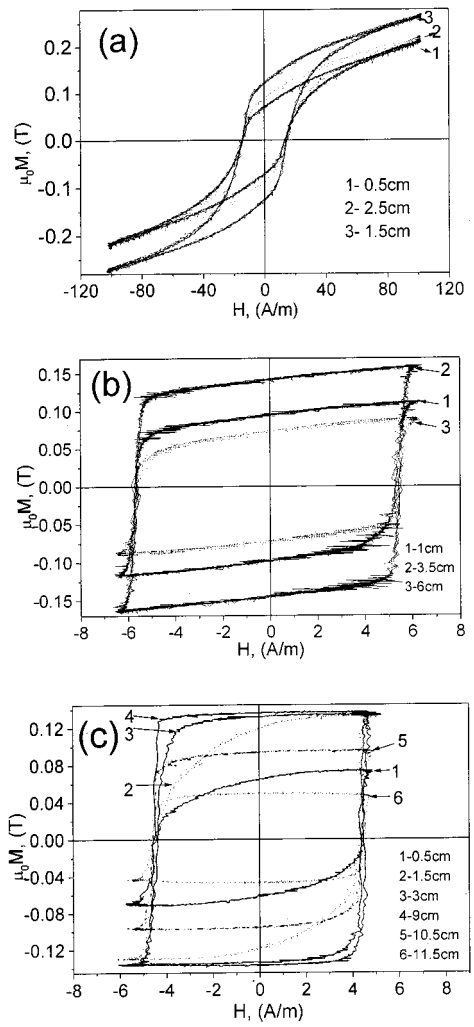

FIG. 2. Local hysteresis loops of $Co_{72.5}Si_{12.5}B_{15}$ amorphous wire measured for sample lengths of 3 (a), 7 (b) and 12 cm (c).

The effect of twisting of the magnetization distribution in the inner core may be described qualitatively by means of a trial function

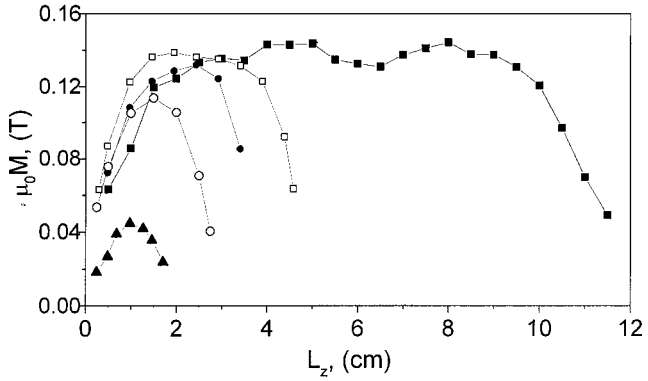

FIG. 3. Magnetization profile of $Co_{72.5}Si_{12.5}B_{15}$ amorphous wire measured for sample lengths of 2, 3, 4, 5, and 12 cm (see notes in the figure).

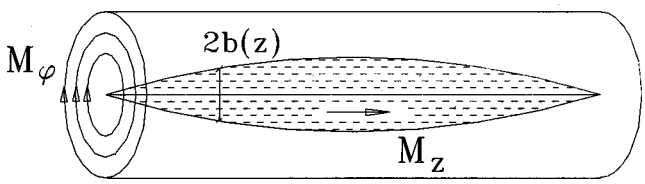

FIG. 4. Schematic picture for magnetization distribution in a short piece of a Co-rich amorphous wire; $b(z)$ is the effective radius of the inner core twisted near the wire ends. The average core magnetization is parallel to the wire axis.

$$\alpha_\rho = 0,$$

$$\alpha_\varphi = \begin{cases} \dfrac{2\rho b(z)}{\rho^2 + b^2(z)}, & \rho < b \\ 1, & \rho > b \end{cases}$$

$$\alpha_z = \sqrt{1-\alpha_\varphi^2}. \tag{2}$$

Here $b(z)$ is the effective radius of a twisted core since in accordance with Eq. (2) at $\rho < b$ the unit magnetization vector has a nonzero α_z component while at $\rho > b$ this component vanishes. For a short piece of wire it seems reasonable to describe the effective core radius by a simple expression

$$b(z) = b_0[1-(2z/L_z)^2]; \quad |z| \leqslant L_z/2, \tag{3}$$

where b_0 is the maximal value of the core radius in the middle of the short wire. It is assumed to be a variational parameter. One may expect that b_0 is an increasing function of the wire length.

Note that for model (3) the effective radius b vanishes at $z = \pm L_z/2$, and therefore the surface magnetic charge is absent at the ends of the wire. Nevertheless there is a volume magnetic charge distributed throughout the inner core with a volume density

$$M_s q(\rho,z) = -M_s \frac{\partial \alpha_z}{\partial z} = \begin{cases} -M_s \dfrac{4b\rho^2}{(b^2+\rho^2)^2}\dfrac{db}{dz}, & \rho \leqslant b \\ 0, & p > b. \end{cases} \tag{4}$$

Thus, for model (3) the surface magnetic charge is scattered into the volume. Further we prove that this leads to a considerable reduction of the magnetostatic energy of the wire. Of course, in a more refined model one may assume that the radius b has a small but nonzero value at the ends of the wire; then some surface charge remains in the domain $\rho < b$. But here we consider only the simple model (3) when the magnetostatic energy of the inner core is given by

$$W_m = \frac{M_s^2}{2}\int d\nu_1 \int d\nu_2 \frac{q(\mathbf{r}_1)q(\mathbf{r}_2)}{|\mathbf{r}_1 - \mathbf{r}_2|}, \tag{5}$$

the integration being throughout the core volume.

Contrary to the magnetostatic energy, the magnetic anisotropy energy of the wire increases due to twisting of the magnetization in the inner core. For simplicity we suppose in this paper that the magnetic anisotropy energy of the inner core is given by the expression

$$W_a = 2\pi K_e \int_{|z| \leqslant L_z/2} dz \int_0^{R_1} \rho\, d\rho\, \alpha_\varphi^2(\rho), \tag{6}$$

where K_e is the average value of the anisotropy constant over the inner core.

We consider also the influence of a weak external magnetic field applied along the wire axis on the magnetization distribution in the inner core of the wire. The increase of the Zeeman energy of the inner core due to magnetization twisting can be evaluated as

$$\Delta W_Z = 2\pi M_s H_0 \int_{|z| \leqslant L_z/2} dz \int_0^{R_1} \rho\, d\rho (1-\alpha_z), \tag{7}$$

H_0 being the amplitude of the uniform external magnetic field.

Since the initial core radius of a Co-rich water-quenched wire is large enough, $R_1 = (2-4)\times 10^{-3}$ cm,[7,8] it is easy to see that the exchange energy contribution to the total core energy is negligibly small. Therefore, the equilibrium value of the parameter b_0 can be determined by means of minimization of the sum of energies (5)–(7).

A. Case of a short wire, $b_0 \leqslant R_1$

At first, let us consider the case of a short enough wire when the equilibrium value of the variational parameter $b_0 \leqslant R_1$. For this case the calculations can be carried out explicitly. Using Eqs. (2) and (3) in Eq. (6) one can evaluate the magnetic anisotropy energy of the inner core as

$$W_a = K_e V_1[1-\xi_a(b_0/R_1)^2], \quad \xi_a = \tfrac{8}{15}(3-4\ln 2), \tag{8}$$

where $V_1 = \pi R_1^2 L_z$ is the core volume.

To evaluate the magnetostatic energy of the wire one should take into account that the core radius is much smaller than the wire length and the function $b(z)$ is very slow. Using the method given in Ref. 23, let us introduce the auxiliary length l such that $R_1 \ll l \ll L_z$ and rewrite the magnetostatic energy (5) as a sum of the contributions

$$W_m = W_m^{(1)} + W_m^{(2)}. \tag{9}$$

Here it is assumed that in the first term on the right-hand side of Eq. (9) the integration is over the domain $|z_1 - z_2| \geqslant 2l$, while in the second term the one is over the domain $|z_1 - z_2| \geqslant 2l$. Taking into account the thickness of the wire one can put approximately $|\overline{r_1} - \overline{r_2}| \approx |z_1 - z_2|$ in the integrand of the first term of Eq. (9). Then, using the reduced charge density corresponding to the unit wire length

$$\overline{q}(z) = 2\pi \int_0^{R_1} \rho\, d\rho\, q(\rho,z) = -4\pi[\ln 2 - \tfrac{1}{2}] b \frac{db}{dz}, \quad b_0 \leqslant R_1, \tag{10}$$

one can rewrite the first term of Eq. (9) in the form

$$W_m^{(1)} = \frac{M_s^2}{2} \int\int_{|z_1 - z_2| \geqslant 2l} dz_1 dz_2 \frac{\overline{q}(z_1)\overline{q}(z_2)}{|z_1 - z_2|}.$$

In the leading approximation this integral can be evaluated as in Ref. 23

$$W_m^{(1)} \approx M_s^2 \int_{|z|\leq L_z/2} dz\, \overline{q}^2(z) \ln \frac{L_z}{2l}. \tag{11a}$$

Next, owing to the condition $|z_1 - z_2| \leq 2l$ one can put in the integrand of the second term of Eq. (9)

$$b(z_1) \approx b(z_2), \quad q(\rho_2, z_2) \approx q(\rho_2, z_1).$$

Besides, averaging the charge density (4) over the core cross section, one may set approximately

$$q(\rho, z) \approx \frac{1}{\pi b^2(z)} \overline{q}(z).$$

Bearing in mind these approximations one can evaluate the second term in Eq. (9) as

$$W_m^{(2)} \approx M_s^2 \int_{|z|\leq L_z/2} dz\, \overline{q}^2(z) \ln \frac{2l}{b(z)}. \tag{11b}$$

We see, therefore, that the sum of the contributions (11a) and (11b) does not contain the arbitrary length l at all. This leads to the relation

$$W_m \approx M_s^2 \int_{|z|\leq L_z/2} dz \overline{q}^2(z) \ln \frac{L_z}{b(z)}. \tag{12}$$

Finally, taking into account the Eqs. (3) and (10), the magnetostatic energy contribution to the total core energy is given by

$$W_m = \xi_m M_s^2 b_0^3 \frac{b_0}{L_z} \ln \frac{L_z}{b_0}, \quad \xi_m = \tfrac{128}{105}[4\pi(\ln 2 - \tfrac{1}{2})]^2. \tag{13}$$

Note, that the magnetostatic energy of a circle of a radius b_0 uniformly charged with the surface density $\sigma = M_s$ is proportional to $M_s^2 b_0^3$. Thus, the scattering of the surface magnetic charge into the volume leads to a considerable reduction of the magnetostatic energy of the inner core due to the small factor $b_0/L_z \ll 1$. Evidently, this is the cause for the twisting of the magnetization in the inner core of the wire.

When an external magnetic field is applied along the wire axis, the Zeeman energy of the inner core must be taken into account too. Using Eqs. (2) and (3) in Eq. (7) one can evaluate this contribution as

$$\Delta W_Z = M_s H_0 V_1 [1 - \xi_H (b_0/R_1)^2], \quad \xi_H = 8(\ln 2 - 0.5)/15. \tag{14}$$

Further we suppose that the field amplitude H_0 is positive when the magnetic field points along the direction of the remanent wire magnetization. In such a case the increase of the magnetic field leads to a corresponding increase of b_0.

Minimizing the sum of energies (8), (13), and (14) with respect to b_0 one can obtain the equilibrium value of this parameter as

$$b_0 = L_z \left[\left(\eta_1 \frac{K_e}{M_s^2} + \eta_2 \frac{H_0}{M_s} \right) \Big/ \left| \ln \left(\eta_1 \frac{K_e}{M_s^2} + \eta_2 \frac{H_0}{M_s} \right) \right| \right]^{1/2}, \tag{15}$$

where the numerical constants are $\eta_1 = \pi \xi_a / 2\xi_m \approx 0.027$ and $\eta_2 = \pi \xi_H / 2\xi_m \approx 0.023$. Therefore, one can see that for the model (3), the core radius near the center of the sufficiently short wire is proportional to the wire length, but the coefficient of proportionality is very small.

Let us define the critical wire length at $H_0 = 0$ by means of the relation $b_0(L_z^*) = R_1$. Then it follows from Eq. (15) that

$$L_z^* = R_1 \left[\frac{M_s^2}{\eta_1 K_e} \ln \frac{M_s^2}{\eta_1 K_e} \right]^{1/2}. \tag{16}$$

Putting $M_s = 500$ emu/cm^3, $K_e = 250$ erg/cm^3, according to Refs. 7 and 8, we see that the ratio $M_s^2/\eta_1 K_e \approx 4 \times 10^4$ is very large, so that we have in this case $L_z^* \approx 600 R_1$. This means that the critical wire length is of the order of several centimeters for a wire with initial core radius $R_1 = (2-4) \times 10^{-3}$ cm.

In the case of $b_0 \leq R_1$ the average longitudinal component of the magnetization of the inner core is given by the equation

$$\frac{\langle M_z \rangle}{M_s} = \frac{2}{R_1^2} \int_0^{b(z)} \rho\, d\rho\, \alpha_z = (2 \ln 2 - 1) \left(\frac{b(z)}{R_1} \right)^2, \tag{17}$$

where $b(z)$ is determined by means of Eqs. (3) and (15). For a remanent state or for a weak enough external magnetic field, Eq. (17) approximately gives the total longitudinal component of the wire magnetization since in this case the outer shell with predominantly circumferential magnetization does not contribute to this quantity considerably. Figure 5(a) shows the reduced z component of the wire magnetization for a short wire as a function of the coordinate z along the wire length as given by Eq. (17). It can be seen that even a weak external magnetic field affects the wire magnetization considerably.

B. Case of a sufficiently long wire $b_0 > R_1$

Consider now the case of a wire with length larger than the critical one, when the equilibrium value of the variational parameter $b_0 > R_1$. Then, in the middle part of the wire, $|z| \leq z_0$, the relation $b(z) > R_1$ holds, while the opposite one is valid near the wire ends, in the intervals $z_0 \leq |z| \leq L_z/2$. Here z_0 is the point where $b(z_0) = R_1$, so that $z_0 = L_z \sqrt{1 - R_1/b_0}/2$. According to Eq. (4), in case of $b_0 > R_1$ Eq. (10) gives the reduced charge density per unit length of the wire in the second interval only, whereas in the interval $|z| \leq z_0$ this quantity is given by

$$\overline{q}(z) = -4\pi b \frac{db}{dz} \left\{ \ln \left[1 + \left(\frac{R_1}{b} \right)^2 \right] - \frac{1}{1 + (b/R_1)^2} \right\}. \tag{18}$$

One must take into account this fact while calculating the magnetostatic energy of the wire by means of Eq. (12). The integration over the z coordinate in Eqs. (6) and (7) should

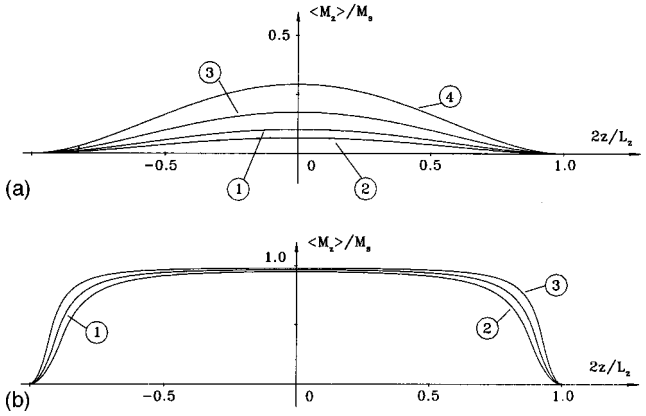

FIG. 5. (a) Axial component of the wire magnetization as a function of the z coordinate for a short amorphous wire with length $L_z=1$ cm ($L_z<L_z^*$) and with initial core radius $R_1=4\times10^{-3}$ cm for various values of external magnetic field: (1) $H_0=0$, (2) $H_0=-0.1$, (3) $H_0=0.2$; (4) $H_0=0.5$ Oe. The mean anisotropy constant in the inner core of the wire and the saturation magnetization are given by $K_e=250$ erg/cm^3 and $M_s=500$ emu/cm^3, respectively. (b). The longitudinal component of the wire magnetization as a function of the z coordinate for an amorphous wire with length $L_z=5$ cm ($L_z>L_z^*$) for various values of external magnetic field: (1) $H_0=0$, (2) $H_0=-0.2$, (3) $H_0=0.5$ Oe. The anisotropy constant, the saturation magnetization, and the initial core radius of the wire are the same as in Fig. 5(a).

be taken separately for these two intervals too. Since the corresponding relations are rather cumbersome, the equilibrium value of the variational parameter in the case considered can be determined by means of the numerical minimization of the sum of the expressions (5)–(7).

In the case of $b_0>R_1$, Eq. (17) gives the average longitudinal component of the wire magnetization in the intervals $z_0\leqslant|z|\leqslant L_z/2$ only. In the middle part of the wire this quantity can be calculated by means of the equation

$$\frac{\langle M_z\rangle}{M_s}=\left(\frac{b}{R_1}\right)^2\left\{2\ln\left[1+\left(\frac{R_1}{b}\right)^2\right]-\left(\frac{R_1}{b}\right)^2\right\}. \qquad (19)$$

The reduced longitudinal component of the wire magnetization for a wire with length larger than the critical one is shown in Fig. 5(b) for different, but small values of external magnetic field. One can see that for a long enough wire this component saturates in the middle part of the wire. As we shall see in the following section, this behavior is in qualitative accordance with the experimental behavior of the longitudinal magnetization in the amorphous Co-rich wire.

Using Eqs. (17) and (19) one can calculate the average remanent magnetization of the wire as a function of its length. The results of these calculations are shown in Fig. 6 for wires with different initial values of the inner-core radius. It should be noted that the critical lengths are given by $L_z^*=1.4$ and 1.85 cm for the curves 1 and 2, respectively. Thus, the critical length defined by Eq. (16) corresponds approximately to the point in Fig. 6, where the remanent wire magnetization increases most rapidly.

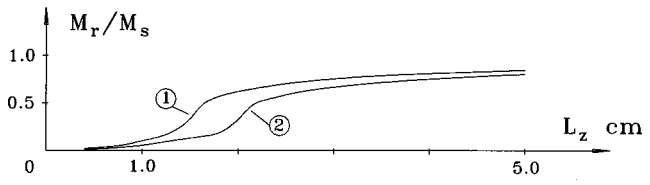

FIG. 6. Remanent magnetization of a Co-rich amorphous wire as a function of the wire length for different initial values of the inner core radius: (1) $R_1=30$, (2) $R_1=40$ μm. The anisotropy constant and the saturation magnetization of the wire are the same as in Fig. 5(a).

In conclusion it is worth to note that the derivation given in this section is not restricted to the simplest model, Eqs. (2) and (3), assumed above for the magnetization behavior near the wire ends. In fact, the estimation (12) for the magnetostatic energy of a thin wire holds for any smooth function $b(z)$ vanishing at the wire ends. Corresponding generalization of the variational procedure gives qualitatively similar results: (1) the longitudinal component of the wire magnetization in the remanent state is a bell-shaped function with a plateau for a long enough wire; (2) the remanent magnetization of the short wire is an increasing function of the wire length.

IV. DISCUSSION AND CONCLUSIONS

Let us compare the theoretical results presented in Sec. III with the experimental data discussed in Sec. II. Assuming the core-shell magnetization distribution within the Co-rich amorphous wire, the radius of the uniformly magnetized core of the wire can be estimated as follows:

$$R_1\approx(M_r/M_s)^{1/2}R, \qquad (20)$$

where M_r is the remanent wire magnetization. To a first approximation, the longitudinal magnetization μ_0M_z of a local part of amorphous wire can be estimated as a value measured at the hysteresis loop just before the large Barkhausen jump. Considering that $\mu_0M_r\approx\mu_0M_z\approx0.14$ T in the central regions of 7- and 12-cm-long wires, one can estimate the inner-core radius as $R_1\approx0.47R=29$ μm for the middle part of a sufficiently long wire. It is worth noting that this result is very close to the theoretical prediction $R_1\approx0.44R$ made for the as-cast Co-rich water-quenched wire.[10] On the other hand, μ_0M_z decreases down to 0.06 T at the distance 0.5 cm from the wire end. Therefore, close to the wire end the inner-core radius is given by $R_1\approx0.31R=19$ μm. This estimation confirms the reduction of the inner-core radius near the wire ends.

Local hysteresis loop measurements permit us to estimate a critical length of the Co-rich amorphous wire experimentally. One can see from Fig. 3 that the longitudinal magnetization of short ($L_z\leqslant3$ cm) samples even in the middle part of the wire is much lower than that of long ($L_z\geqslant4$ cm) samples. This means that the effect of the demagnetizing field on the longitudinal magnetization in the middle part of the wire becomes negligible for a wire with $L\geqslant4$ cm. Therefore the critical length of the Co-rich wire with D

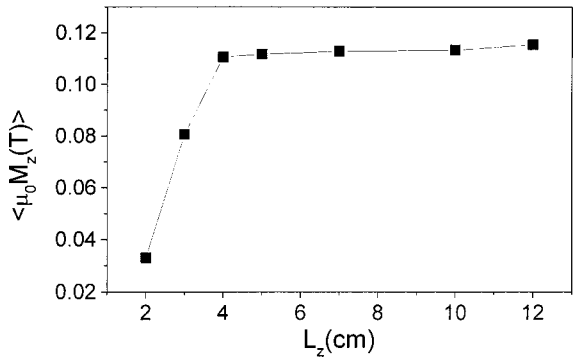

FIG. 7. Experimental dependence of average longitudinal magnetization $\langle \mu_0 M_z \rangle$ on the sample length.

$=125\ \mu$m can be estimated to be about 4 cm. To confirm this estimation an average axial magnetization $\langle \mu_0 M_z \rangle$ has been determined from measured magnetization profiles for samples with different length. The corresponding length dependence of average axial magnetization is presented in Fig. 7. One can see that experimentally $\langle \mu_0 M_z \rangle$ strongly increases with L for $L<4$ cm and becomes almost independent on L for $L \geqslant 4$ cm. Therefore, the experimental results for the Co-rich wire are in good qualitative agreement with the theoretical model described in Sec. III (see Fig. 6).

According to above estimation the critical length of Co-rich wire is approximately one-half of that of the Fe-rich wire. Probably, this difference is related to the lower value of saturation magnetization of the Co-rich wire (0.64 T comparatively to 1.5 T for the Fe-rich wire) and with smaller diameter of the inner axially magnetized core for the Co-rich wire. Actually, the reduced remanent magnetization is typically $M_r/M_s \approx 0.5$ for Fe-rich samples and only about 0.22 for Co-rich wires. Besides, the different sign and value of the magnetostriction constant result in a significant difference of the outer shell domain structure. In reality this difference might cause different domain structure of the end domains in Co-rich wires. Consequently, the critical length to observe magnetic bistability should be also different.

In conclusion, in this paper a proper generalization of the core-shell model is developed for a Co-rich amorphous wire of a finite length. It is well known that for a sufficiently long Co-rich amorphous wire the core-shell model explains naturally most of the existing experimental data.[1,3,8] Recently it was stated also that the core-shell magnetization configuration is a consequence of a radial dependence of the residual stress tensor components of amorphous wire.[10] The estimation[3] based on the value of the remanent wire magnetization shows that for a typical water-quenched 125-μm-diameter Co-rich wire the radius of the inner core, uniformly magnetized along the wire axis, turns out to be rather large $R_1=(2-4)\times 10^{-3}$ cm. In such a case the demagnetizing field of surface magnetic charges arising near the wire ends can disturb considerably the magnetization distribution near the wire ends. In this paper, we show that the magnetostatic energy of the magnetic charges can be reduced by means of twisting the magnetization in the core region near the wire ends. In our case, the critical length for the magnetization twisting turns out to be several orders larger than the wire radius. In addition, it follows from the model that, for a short piece of wire with a length lower than the critical one, the total remanent magnetization is an increasing function of the wire length. Both of the theoretical predictions seem to be in qualitative agreement with the present experiment, though further investigations are necessary to understand the remagnetization process of a short piece of a Co-rich wire in detail.

*On leave of the Donostia International Physics Center, P. M. De Lardizabal, 4, 20018, San Sebastian, Spain.

[1] P. T. Square, D. Atkinson, M. R. J. Gibbs, and S. Atalay, J. Magn. Magn. Mater. **132**, 10 (1994).
[2] M. Vazquez and D. X. Chen, IEEE Trans. Magn. **31**, 1229 (1995).
[3] M. Vazquez and A. Hernando, J. Phys. D **29**, 939 (1996).
[4] K. Mohri, T. Kohzawa, K. Kawashima, H. Yoshida and L. V. Panina, IEEE Trans. Magn. **28**, 3150 (1992).
[5] R. S. Beach and A. E. Berkowitz, Appl. Phys. Lett. **64**, 3652 (1994).
[6] F. B. Humphrey, K. Mohri, J. Yamasaki, H. Kawamura, R. Malmhall, and J. Ogasawara, in *Magnetic Properties of Amorphous Metals*, edited by A. Hernando *et al.* (Elsevier, Amsterdam, 1987).
[7] K. Mohri, F. B. Humphrey, K. Kawashima, K. Kimura, and M. Mizutani, IEEE Trans. Magn. **26**, 1789 (1990).
[8] J. M. Blanco, P. Aragoneses, E. Iririeta, J. Gonzalez, and K. Kulakowski, J. Appl. Phys. **75**, 6315 (1994).
[9] K. Kulakowski, J. Gonzalez, and P. Aragoneses, J. Magn. Magn. Mater. **162**, 255 (1996).
[10] A. S. Antonov, V. T. Borisov, O. V. Borisov, V. A. Pozdnyakov, A. F. Prokoshin, and N. A. Usov, J. Phys. D **32**, 1788 (1999).
[11] R. M. Cristensen, *Theory of Viscoelasticity: An Introduction* (Academic, New York, 1971).
[12] S. V. Vonsovsky, *Magnetism* (Moscow, Nauka, 1971).
[13] N. Usov, A. Antonov, A. Dykhne, and A. Lagar'kov, J. Phys.: Condens. Matter **10**, 2453 (1998).
[14] A. M. Severino, C. Gomez-Polo, P. Marin, and M. Vazquez, J. Magn. Magn. Mater. **103**, 117 (1992).
[15] T. Reininger, H. Kronmuller, C. Gomez-Polo, and M. Vazquez, J. Appl. Phys. **73**, 5357 (1993).
[16] D. X. Chen, C. Gomez-Polo, and M. Vazquez, J. Magn. Magn. Mater. **124**, 262 (1993).
[17] A. P. Zhukov, M. Vázquez, J. Velázquez, H. Chiriac, and V. Larin, J. Magn. Magn. Mater. **151**, 132 (1995).
[18] A. Zhukov, J. Velázquez, E. Navarro, and M. L. Sanchez, in *Nanostructured and Non-crystalline Solids*, edited by M. Vazquez and A. Hernando, (World Scientific, Singapore, 1995), pp. 542–546.
[19] M. E. Shabes, J. Magn. Magn. Mater. **95**, 249 (1991).
[20] Y. D. Yan and E. Della Torre, J. Appl. Phys. **66**, 320 (1989).
[21] N. A. Usov, J. Magn. Magn. Mater. **203**, 277 (1999).
[22] S. Hirono, K. Nonaka, and I. Hatakeyama, J. Appl. Phys. **60**, 3661 (1986).
[23] L. D. Landau and E. M. Lifshitz, *Electrodynamics of Continuous Media*, 2nd ed. (Pergamon, New York, 1984).